Thermal and geometric properties of alloy clusters studied with Brownian-type isothermal molecular dynamics simulations

Tsung-Wen Yen and S. K. Lai*
Complex Liquids Laboratory, Department of Physics, National Central University, Chungli 320, Taiwan Republic of China

N. Jakse† and J. L. Bretonnet
Laboratoire de Physique des Milieux Denses University Paul Verlaine Metz, 1, Boulevard F.D. Arago, 57078 Metz, Cedex 3, France
(Received 22 October 2006; revised manuscript received 12 January 2007; published 30 April 2007)

We report a Brownian isothermal molecular dynamics simulation study of bimetallic clusters. Beginning at their lowest energy structures which were obtained from a recently developed algorithm [P. J. Hsu and S. K. Lai, J. Chem. Phys. **124**, 044711 (2006)], we investigate the effect of temperature on the thermal and geometric of Cu_mAu_{n-m} at given nuclearity n. We study in particular the change in temperature of the relative root-mean-squared bond length fluctuation δ so-called Lindemann parameter and exploit the underlying mechanism that leads to its thermal variation. We then discuss the correlation of δ to the specific heat which is used generally to deduce the bulklike melting of bimetallic clusters. The mismatch quite often seen at the melting temperature between δ and specific heat can now be understood better.

DOI: 10.1103/PhysRevB.75.165420 PACS number(s): 61.46.Bc, 82.20.Wt, 36.40.Qv

I. INTRODUCTION

The bimetallic clusters have received much focus in recent years. Structurally, the bimetallic cluster (BC) exhibits many characteristic features which are absent in its pure counterparts. The alloying properties of segregation and mixing are two most obvious features. In the former, metallic atoms of one species bond together in a certain region or form layers well separated from atoms of the other species, whereas in the latter metallic atoms of one species distribute to have atoms of the other species as their neighbors. The number composition dependence of a BC has thus been taken as one important variable in understanding its structural stability.

In the context of determining the ground-state structure, there has been impressive progress. López *et al.*[1] investigated the structural properties of Cu_aAu_b (hereafter a cluster size is denoted by $n=a+b$) using the thermal quenching procedure. Limited to sizes $n=13$ and 14, they predicted that the lowest energy geometries of these BCs prefer icosahedral structures for *all* stoichiometric compositions despite the fact that the lowest energy structure of pure Au_{14} takes on a centered hexagonal antiprism with one atom occupying one of its bases (pure clusters Cu_{13}, Cu_{14}, and Au_{13} all assume icosahedral or icosahedron-derived structures). Terminologically, these authors classified the structures of a BC into two categories, namely, the topological isomers corresponding to the manifold of geometric forms and the permutational isomers corresponding to different arrangements in the relative positions of the two kinds of atoms for a fixed topological structure. Similar calculations for the Ni_aAl_b of size $n=13$ have been reported independently by Rey *et al.*[2] and Krissinel and Jellinek.[3,4] Rey *et al.* employed the Voter and Chen version of the embedded-atom model[5] to account for the many-body interactions between atoms whereas Krissinel and Jellinek used instead the same Gupta-like potential model[6,7] as López *et al.*[1] The predicted lowest energy structures for $Ni_{12}Al_1$ by these two groups are topologically the same, i.e., $Ni_{12}Al_1$ takes on an icosahedral structure, but the predicted permutational isomers are, however, in contradiction. Rey *et al.* found the central atom in the icosahedron to be the Ni atom whereas Krissinel and Jellinek[4] predicted the Al atom sitting at the central site. Two years later, Calleja *et al.*[8] reexamined this disparity using a fully self-consistent density functional technique. The calculation of Calleja *et al.* indicated the discrepancy to originate from the electronic contribution, but their analysis implied also that the disagreement might be due to the use of different semiempirical potentials. Three years later, Rexer *et al.*[9] analyzed experimentally the reactions of N_2 with the surface atoms in Ni_aAl_b and concluded speculatively that the central atom in the icosahedron of $Ni_{12}Al_1$ is *probably* the Ni atom. Subsequently, theoretical efforts were seen to shift to developing techniques that are capable of finding ground-state structures of BCs having larger size.[10–17]

In spite of this impressive progress on the studies of ground-state structures, much less attention is paid to investigating the thermal properties of BCs. López and Freeman[18] presented one of the earlier works on the thermal behavior of BC using the *J*-walking Monte Carlo (MC) method. They found in their heat capacity results for Pd_6Ni_7 that this cluster displays an anomalous low temperature peak which has been interpreted as signaling a isomerization transition involving permutational isomers. Soon after the latter simulation work, López *et al.*[1] reported constant energy simulation studies of Cu_aAu_b for a series of dynamic quantities. Contemporaneously, Krissinel and Jellinek[4] studied the thermal properties of Ni_aAl_b by employing the same microcanonical molecular dynamics (MD) method as López *et al.*[1] Calculations by these authors were confined to $n=13$ and 14. Since then, published works on the thermodynamic and dynamic properties of BCs are relatively scarce. Apart from the studies of the thermal behavior for Cu-Ni by Huang and Balbuenawas[19] three years ago, it is only very recently that one sees simulation works on the temperature effects of BCs for Au-Ag,[20] Pd-Pt,[21] and Cu-Au.[22]

It is the purpose of this paper to extend our recent thermal studies of pure metallic clusters[23] to BCs. First, we shall touch on one feature intimately connected with the MD simulations which were performed mostly in the context of microcanonical ensemble. The feature is that it is not clear if current simulation results, in particular for BCs, are quantitatively dependent on the thermodynamic ensemble used. There is indication in a previous model calculation[24] that for finite systems the results obtained in a microcanonical ensemble differ from other ensembles, for instance, the canonical ensemble. The second feature that we shall delve into is to study the mechanisms of melting in BCs, since structural portraits of BCs have the possibilities of undergoing isomerization transition involving permutational as well as topological isomers. We shall calculate the relative root-mean-squared (rms) bond length fluctuation δ and the caloric curve of specific heat C_V which are two quantities often used in bulk systems for shedding light on melting. To ensure a correct description of the thermal characteristics of BCs, an accurate ground-state atomic configuration and an efficient simulation algorithm for studying thermal properties are the ingredients of success. For the former, we calculate the lowest energy structures of BCs using an extremely stable, accurate and reliable algorithm recently developed by us[17] for BCs. This algorithm is based on the genetic algorithm and the MC-based basin hopping method which are two state-of-the-art techniques widely applied to predict the ground-state structures of many different kinds of clusters, both metallic and nonmetallic. For the latter, we prefer the Brownian-type isothermal MD scheme since the method has previously been tested by us to be satisfactory for pure metallic clusters.[23] Although the generalization of the same methodology to BCs is conceptually straightforward, it is of pedagogical interest, however, to review this efficient algorithm, albeit briefly, and make a few remarks on its relevance to other similar schemes. Let us recall, in the first place, that we are interested in the response of a free cluster to thermal probe. It is therefore necessary to stipulate its temperature. A possible means is to arrange the cluster in thermal contact with a heat bath that is maintained at the desired temperature. Inspired by the works of Nosé[25] and Hoover,[26] Kusnezov *et al.*[27] simulated the coupling to a heat bath by introducing pseudofriction terms in a cubic coupling scheme (CCS). According to these authors one of the principal difficulties of the Nosé-Hoover method is its unpredictability of the condition of ergodicity and the method has in addition the drawback of strongly depending on the initial conditions, algorithm parameters and forms of the pseudofriction terms. As demonstrated numerically for a few simple model systems,[27] the CCS with the introduced pseudofriction coefficients is devoid of most of these flaws and the scheme is indeed an efficient algorithm (better than the Nosé-Hoover approach). The CCS is particularly appealing since it ensures ergodicity and allows a relatively fast exploration of the phase space. Nevertheless, there remains an unsatisfactory feature when the CCS was applied to study metallic clusters. Bulgac and Kusnezov[28] have, in fact, shown that the coupling coefficients in the CCS depend upon the size of cluster as well as the temperature at which the cluster is maintained. The technical difficulty is that, in the study of a large cluster especially at a high temperature, one must employ a relatively small time step in the simulation run. A modification to the CCS similar to the description of a Brownian particle[29] was subsequently proposed by Ju and Bulgac.[30] This modified version of the CCS which will be used below remedies the aforementioned deficiencies by prescribing the optimal coupling coefficients to depend explicitly on the temperature and cluster size. The algorithm has in fact been critically tested by them and more recently by us[23] and it has been shown to work pretty well for large clusters in a wide range of temperatures. One practical reason that makes the modified CCS attractive is that almost the same time step of integration may be used for most of the clusters of interest. As in the case of CCS, this modified scheme also shows a fast exploration rate of the ergodic phase space.

In addition to the technical aspects indicated above, we should perhaps remark furthermore that the modified CCS is not the only choice that one can use for controlling the thermal fluctuations in a thermally driven n-body system. Equally promising schemes have been reported as well. We draw attention, in particular, to the technique of multiple thermostats since the latter has the same ultimate goal as the CCS which aims at sampling from the canonical ensemble. Implementing multiple thermostats in MD simulations has accordingly received much attention in the literature. In one of the earlier works, Martyna *et al.*[31] applied the idea of multiple thermostats to study the harmonic oscillator and the one dimensional free particle and they found that for these systems it works better than the CCS;[27] no parallel comparison with the modified CCS has, however, been reported. In view of the simulations results of Martyna *et al.*, the use of multiple thermostats to study the thermal behavior of an n-body system is certainly an alternative to the modified CCS, even though this kind of multiple thermostatting method needs still to be further evaluated[32] as pointed out in a very recent article by Leimkuhler and Sweet[33] who proposed a Hamiltonian formulation to construct the so-called recursive multiple thermostats within the context of the Nosé-Poincare method.[34] The implementation and application of this latter scheme and a comparison of it with the modified CCS for studying the thermal behavior of metallic clusters would be a challenging endeavor. Here, for the purpose of assessing further the salient features of the modified CCS and for comparison with theoretical studies obtained by others, we shall present results of Cu_mAu_{n-m}, $n=13$ and 14.

The present work is organized as follows. In the next section, we give a brief account of the computational details which consist of describing the many-body potential and the use of it in the Brownian-type isothermal MD simulation. We shall present and analyze, in Sec. III, the temperature variation of Cu_mAu_{n-m} appealing, in particular, to an instantaneous bond length whose temporal development at given temperature permits deeper understanding of the microscopic dynamics of pair of atoms (within the n-atom cluster) of the same and different kinds. A summary of our main findings is given in Sec. IV.

II. COMPUTATIONAL DETAILS

In this section, we introduce briefly the many-body potential and describe how it was used in the Brownian-type isothermal MD.

TABLE I. Time step Δt, equilibrium time t_{eq}, and total elapsed time t_{tot} for Cu_mAu_{n-m} at nuclearities $n=13$ and 14.

Bimetallic cluster	Δt (fs)	t_{eq} (ns)	t_{tot} (ns)
Au_{13}	5	25	100
Cu_1Au_{12}	1	10	100
Cu_6Au_7	0.5	10	100
Cu_7Au_6	1	10	100
$Cu_{12}Au_1$	1	10	200
Cu_{13}	5	25	100
Cu_{14}	5	25	100
Cu_1Au_{13}	1	10	100
Cu_7Au_7	0.5	10	100
$Cu_{13}Au_1$	1	10	100
Au_{14}	5	25	100

A. Gupta-type potential

In a finited-sized BC, in order to account for the interactions between the Cu and Au atoms which are intrinsically many-body in nature, we employ the widely used n-body Gupta potential.[7,35] This empirical potential can be written

$$E_n = \sum_{i=1}^{n} \left(\sum_{j=1(j\neq i)}^{n} A_{ij} \exp\left[-p_{ij}\left(\frac{r_{ij}}{r_{ij}^{(0)}} - 1 \right) \right] - \left\{ \sum_{j=1(j\neq i)}^{n} \xi_{ij}^2 \exp\left[-2q_{ij}\left(\frac{r_{ij}}{r_{ij}^{(0)}} - 1 \right) \right] \right\}^{1/2} \right), \quad (1)$$

where A_{ij}, ξ_{ij}, p_{ij}, q_{ij}, and $r_{ij}^{(0)}$ are parameters fitted to bulk measured data of cohesive energy, lattice constant, and elastic constants for the face-centered-cubic crystalline structure at 0 K. There are three sets of parameters of which two sets are homonuclear ($i=j$), one for Cu-Cu and the other for Au-Au, and the third set is heteronuclear ($i\neq j$) for Cu-Au. The former sets are adjusted to bulk data taken from the pure Cu and Au metals and are assumed the same in the BC; the latter set is determined by fitting to the crystalline structure of an intermetallic compound. In this work, we use the values of the parameters given by Cleri and Rosato.[7] We refer the interested readers to Ref. 7 for further details.

B. Methodology of the simulations

Having introduced the n-body Gupta-type potential, we proceed to describe the Brownian-type isothermal MD method and the generalization of it to the BC. As stated in the Introduction, we employ the modified CCS which is readily generalized to an alloy cluster $A_{n_a}B_{n_b}$ where n_a (n_b) is the number of atoms of a type (b type). Explicitly, the equations of motion (for the x component) can be written

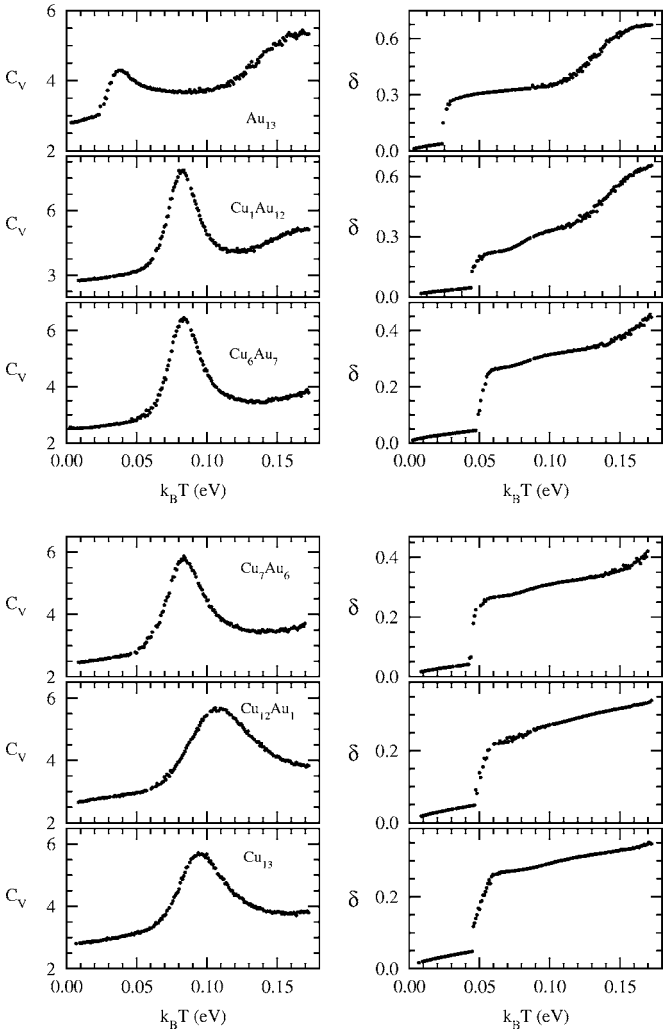

FIG. 1. Constant volume specific heat C_V (in units of k_B) and relative rms bond length fluctuation parameter δ vary with k_BT (eV) for clusters Au_{13}, Cu_1Au_{12}, Cu_6Au_7, Cu_7Au_6, $Cu_{12}Au_1$, and Cu_{13}.

$$\dot{x}_{i(a)} = \frac{p_{i(a),x}}{m_a}, \quad (2)$$

$$\dot{p}_{i(a),x} = -\frac{\partial E_n}{\partial x_{i(a)}} - \frac{\alpha_a e_{0,a}}{nL_0}\mu_{a,x}^3 \frac{p_{i(a),x}}{p_{0,a}} - \frac{\beta_a e_{0,a}}{nL_0}\nu_{a,x}\left(\frac{p_{i(a),x}^2}{p_{0,a}^2} - d_0 \right) - \frac{\varkappa_a e_{0,a}}{nL_0}\eta_{a,x}\frac{p_{i(a),x}^3}{p_{0,a}^3}, \quad (3)$$

in which the subscript $i(a)$ refers to the ith atom of a type, and $\mu_{a,x}$ $\nu_{a,x}$, and $\eta_{a,x}$ are to be determined from

$$\dot{\mu}_{a,x} = \frac{\alpha_a T}{p_{0,a}L_0}\left(\frac{\sum_{i=1}^{n_a} p_{i(a),x}^2}{nm_aT} + \frac{\sum_{i=1}^{n_b} p_{i(b),x}^2}{nm_bT} - 1 \right), \quad (4)$$

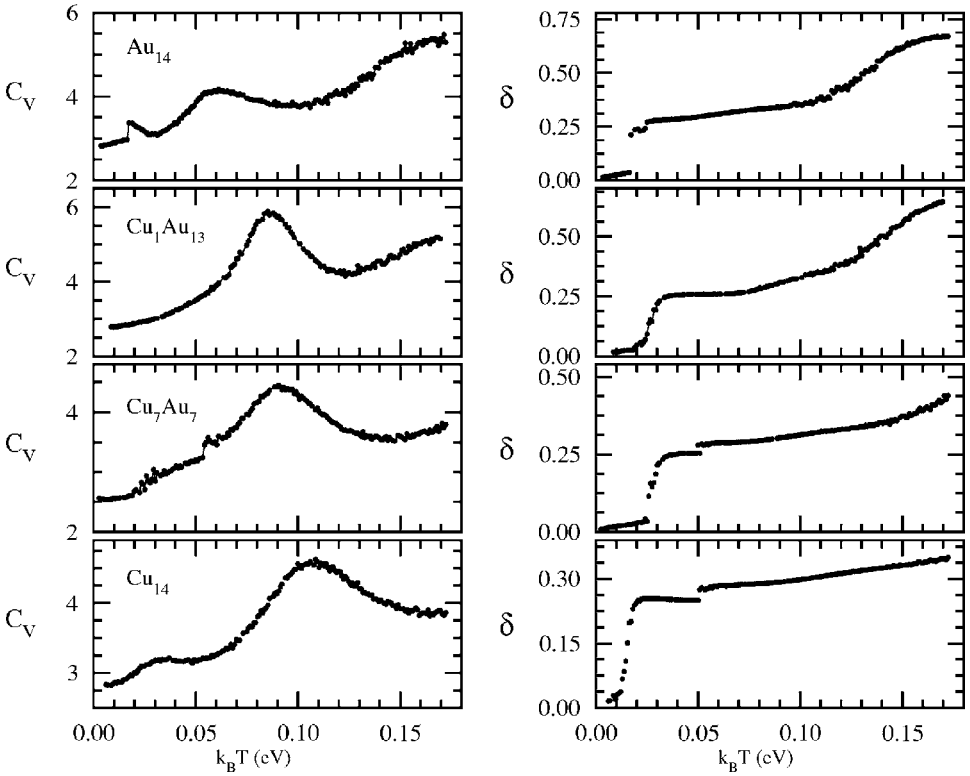

FIG. 2. Constant volume specific heat C_V (in units of k_B) and relative rms bond length fluctuation parameter δ vary with k_BT (eV) for clusters Au_{14}, Cu_1Au_{13}, Cu_7Au_7, and Cu_{14}.

$$\dot{\nu}_{a,x} = \frac{\beta_a T}{p_{0,a} L_0}\left(\frac{\sum_{i=1}^{n_a} p_{i(a),x}^3}{n m_a T p_{0,a}} + \frac{\sum_{i=1}^{n_b} p_{i(b),x}^3}{n m_b T p_{0,b}} - d_0 \frac{\sum_{i=1}^{n_a} p_{i(a),x} p_{0,a}}{n m_a T} - d_0 \frac{\sum_{i=1}^{n_b} p_{i(b),x} p_{0,b}}{n m_b T} - \frac{2\sum_{i=1}^{n_a} p_{i(a),x}}{n p_{0,a}} - \frac{2\sum_{i=1}^{n_b} p_{i(b),x}}{n p_{0,b}}\right) \quad (5)$$

$$\dot{\eta}_{a,x} = \frac{\varkappa_a T}{p_{0,a} L_0}\left(\frac{\sum_{i=1}^{n_a} p_{i(a),x}^4}{n m_a T p_{0,a}^2} + \frac{\sum_{i=1}^{n_b} p_{i(b),x}^4}{n m_b T p_{0,b}^2} - \frac{3\sum_{i=1}^{n_a} p_{i(a),x}^2}{n p_{0,a}^2} - \frac{3\sum_{i=1}^{n_b} p_{i(b),x}^2}{n p_{0,b}^2}\right). \quad (6)$$

In Eqs. (2)–(6), $x_{i(a)}$ and $p_{i(a),x}$ are the x-component position coordinate and momentum, respectively. For b-type atoms, we simply replace the subscript $a \rightarrow b$ in Eqs. (2)–(6). The same set of equations hold for the y and z components. In Eq. (3), E_n is the potential energy defined by Eq. (1), and $\mu_{a,x}$, $\nu_{a,x}$ and $\eta_{a,x}$ are the x-component pseudofriction coefficients of a-type atoms introduced to simulate the heat bath degrees of freedom.[25,36] m_a and $p_{0,a}=\sqrt{2m_aT}$ are the atomic mass and average thermal momentum at temperature T of an a-type atom, respectively, and d_0 is a dimensionless constant with a value of the order of 1. L_0 is also a constant with the dimension of length and numerically its value is of the order of 1 Å. The quantity $e_{0,a}$, which first appears in the time dependent canonical distribution,[27] is an energy constant whose value can be estimated as $e_{0,a} \sim m_a L_0^2 \omega_D^2/(4\pi^2)$. The magnitude of $e_{0,a}$ is thus of the order corresponding to a free cluster exhibiting a Debye frequency ω_D. Lastly, $\alpha_a \sim \beta_a \sim \varkappa_a \sim [m_a L_0^2/(n T t_0^2)]^{1/2}$, in which $t_0 = 2\pi/\omega_D$ is the smallest characteristic time scale of the system, are cluster independent constants.

Considering the kind and the size of BCs to be studied in this work, we have experimented different ranges of values for the aforementioned constant parameters and finally arrived at an optimized set of values. They are $L_0 = 1$ Å, $d_0 = 1$, and $\omega_D = 60 \times 10^{12}$ s^{-1}. Although another choice of these constants is possible, the quality of the simulation results

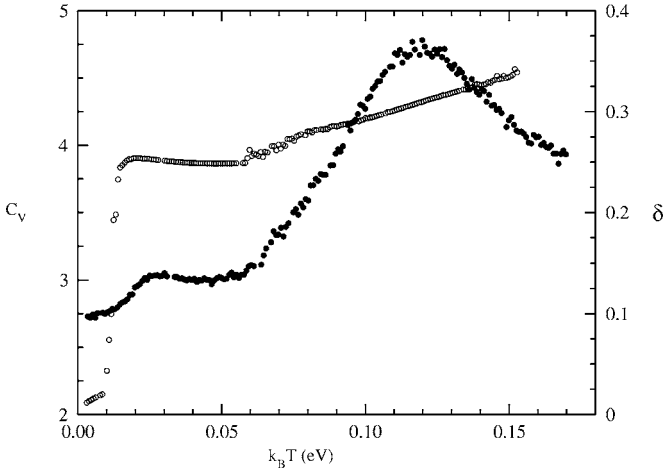

FIG. 3. Constant volume specific heat C_V (in units of k_B) and relative rms bond length fluctuation parameter δ vary with k_BT (eV) for clusters $Cu_{13}Au_1$.

TABLE II. Position T_δ of the relative rms bond length fluctuation parameter δ (see text) and two T_{melt} for the bimetallic clusters Cu_mAu_{13-m} and Cu_mAu_{14-m}.

Cu_mAu_{13-m} m	T_δ (Ref. 1)	T_δ	k_BT_{melt} (eV) (Ref. 1)	k_BT_{melt} (eV)
13	0.07	0.046		
12	0.075	0.048		
7	0.075	0.042		
6	0.075	0.048	0.083	0.082
1	0.072	0.044		
0	0.04	0.025		
Cu_mAu_{14-m} m				
14	0.023	0.009		
13	0.022	0.01		
7	0.036	0.025	0.05/0.09	0.054/0.09
1	0.038	0.019		
0	0.032	0.018		

would not be affected providing that the simulations are performed at long enough times. In this work, the equations of motion were integrated numerically using the Hamming predictor-corrector method of fourth order. With the chosen set of parameters, this integration algorithm allows a larger time step (up to $\Delta t=10^{-14}$ s) to be used. At each T, the simulation run was carried out for at least 0.2×10^8 steps. Much longer simulation time of $6-10\times10^7$ steps was performed for clusters in the temperature region showing the premelting-like feature and in the meltinglike transition region. The total elapsed time t_{tot} for each MD run was therefore $t_{\text{tot}}\geqslant1\times10^{-7}$ s. In actual simulations, we found that $\Delta t=1-5\times10^{-15}$ s is generally sufficient for the quantities studied here. There were, however, exceptional cases where larger fluctuations were encountered. When any of the latter happens, using $\Delta t\leqslant0.5\sim1\times10^{-15}$ s in the MD simulation normally will improve the simulation results. The time step $\Delta t\leqslant0.5-1\times10^{-15}$ s works well also in the lower temperature region ($T<100$ K). As regards the temperature increment, we run the MD simulation at an interval of 5 K in the premelting and meltinglike regions, and at an interval of 10 K in all other regions. Table I gives more details of the time steps used and the total elapsed times in simulations. These data were applied below to study the thermal and geometric properties.

C. Thermal and geometric properties

For the thermal property, we calculated the specific heat C_V. The computation of this quantity is straightforward since the configuration energies were readily recorded by the above equations. Explicitly

$$C_V(T)=\frac{\langle E_{\text{total}}^2\rangle_t-\langle E_{\text{total}}\rangle_t^2}{k_BT^2} \tag{7}$$

where $E_{\text{total}}=(\Sigma_{i(a)}p_{i(a)}^2/(2m_a)+\Sigma_{i(b)}p_{i(b)}^2/(2m_b))+E_n$. A cluster at T is heated up from its zero temperature configuration until it transforms into a liquidlike cluster. We have performed rather long simulation time ($1-3\times10^{-7}$ s) so that the calculated C_V vs T curves develop as smooth as possible. Any larger fluctuation that still remains would indicate the necessity to improve the coupling scheme.

The geometric quantity of interest here is the relative rms bond length fluctuation δ. This quantity dictates the geometric property and is defined by

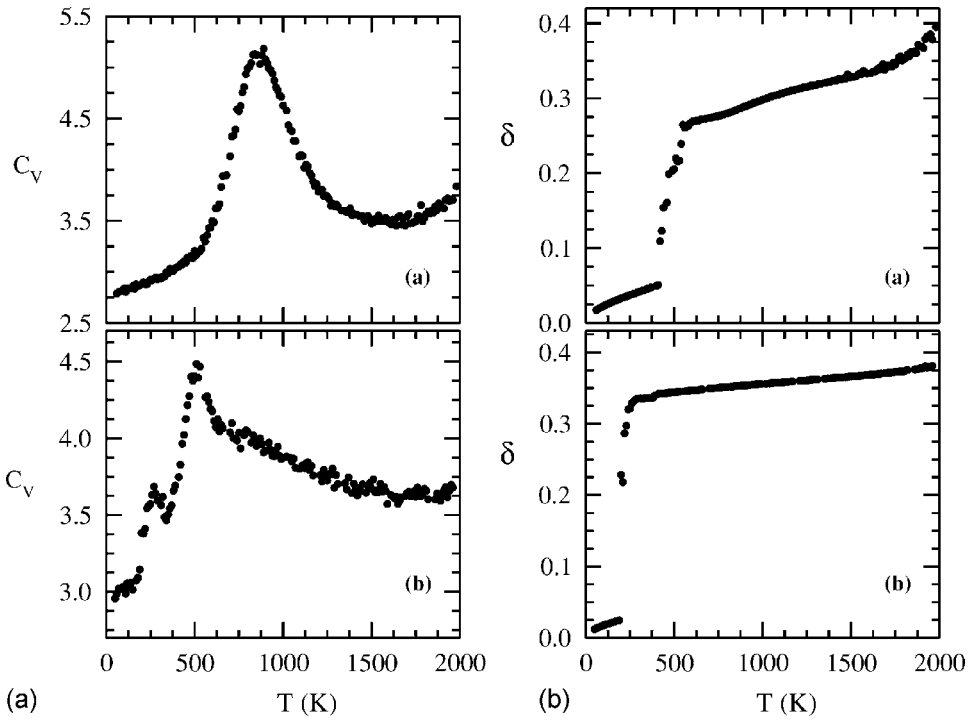

FIG. 4. Constant volume specific heat C_V (in units of k_B) and relative rms bond length fluctuation parameter δ obtained by the Brownian MD simulations for (a) Al_{13} and (b) Al_{58} as a function of temperature T (in units of K). These results should be compared with canonical simulations of Werner (Ref. 38) and Noya *et al.* (Ref. 39).

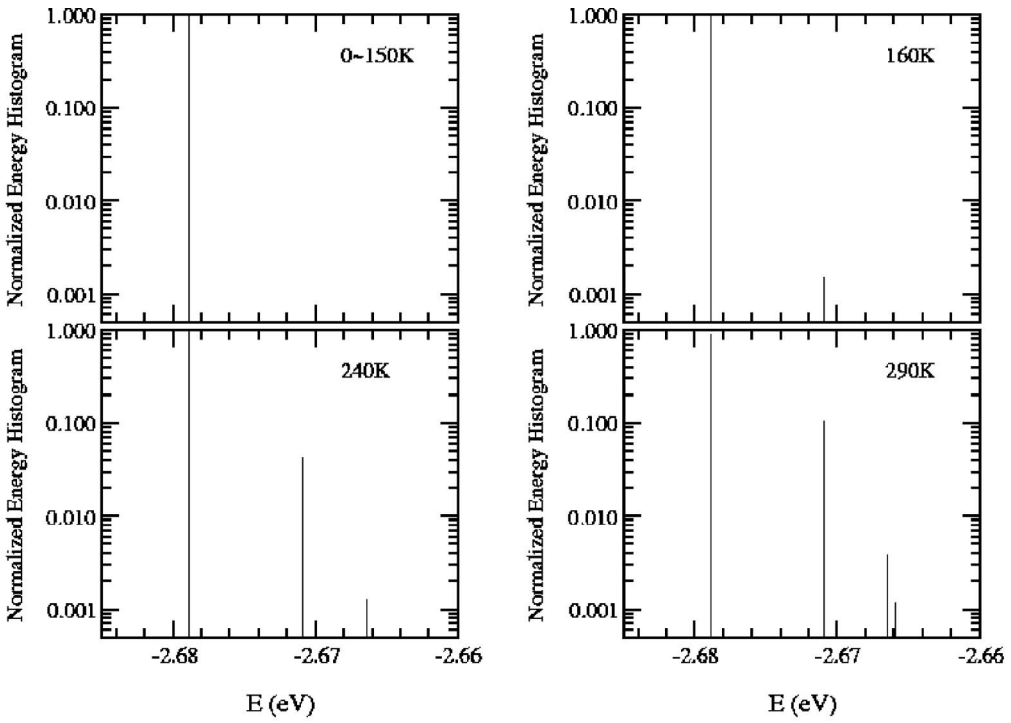

(a) Lowest energy isomer (b) 1st low-lying energy isomer (viewed in two directions)

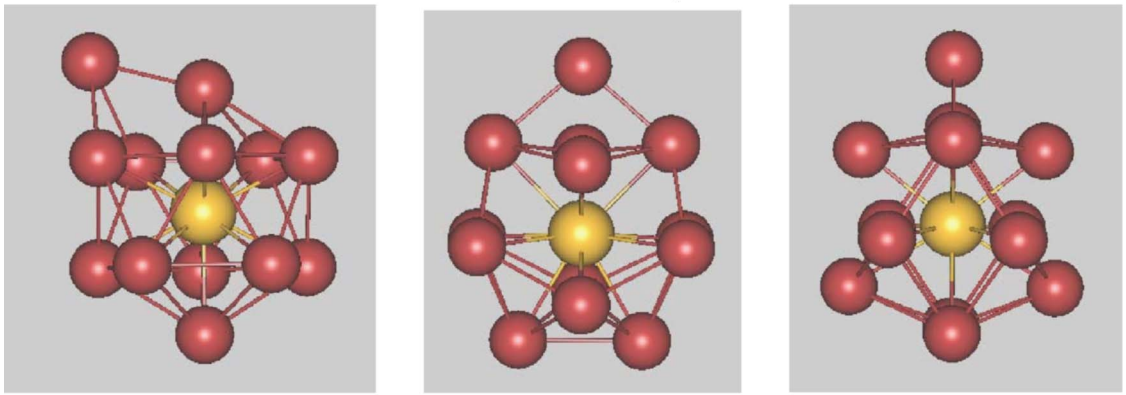

(c) 2nd low-lying energy isomer (d) 3rd low-lying energy isomer

FIG. 5. (Color online) Energy histograms of $Cu_{13}Au_1$ obtained from Brownian MD simulations at temperatures $T=0-150$, 160, 240, and 290 K for (a) the lowest energy isomer, (b) first low-lying energy isomer, (c) second low-lying energy isomer, (d) third low-lying energy isomer.

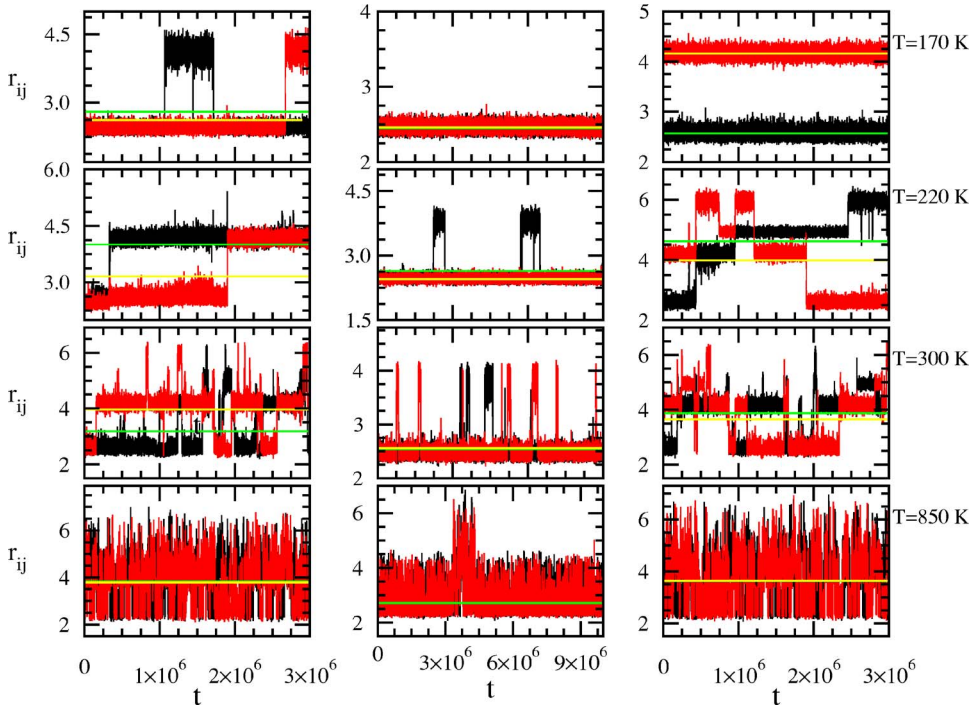

FIG. 6. (Color online) Temporal evolution of the instantaneous bond length $r_{ij}(t)$ vs t (in units of $\Delta t=1\times10^{-15}$) [see Eq. (9)] calculated from Brownian MD simulations for $Cu_{13}Au_1$ at several fixed temperatures. The left column describes $r_{ij}(t)$ with the ith and jth chosen from two Cu surface atoms one of which is the "floating" atom numbered 12 (black: atoms 12 and 7; red: 12 and 10) labeled as in Fig. 7(a), middle column from two atoms one of which is the central atom Au (black: atoms 14 and 8; red: atoms 14 and 6) labeled as in Fig. 7(a), and right column from two surface atoms Cu (black: atoms 3 and 1; red: atoms 3 and 9) labeled as in Fig. 7(a). The horizontal lines (green for black r_{ij} and yellow for red r_{ij}) in each figure refer to $\langle r_{ij}(t)\rangle_t$. When the cluster undergoes permutational transition, $r_{ij}(t)$ deviates more from $\langle r_{ij}(t)\rangle_t$ and is manifested by a up or down step and for each step there is a *positive* contribution to δ. Up to $T=300$ K only permutational transition involving isomers between Cu atoms (all columns) are visualized and at these same temperatures no permutation between Cu and Au atoms is detected [see Fig. 7(a)]. Permutational transition involving isomers between Cu and Au atoms (middle column) are observed at $T=850$ K [Fig. 7(b)]. The time in the middle column is from $t=0$ up to 3×10^6 for the first three rows (from top) whereas the last row is self-explanatory.

$$\delta=\frac{1}{n(n-1)}\sum_{i=1}^{n}\sum_{j\neq i}^{n}\frac{\sqrt{\langle r_{ij}(t)^2\rangle_t-\langle r_{ij}(t)\rangle_t^2}}{\langle r_{ij}(t)\rangle_t}. \tag{8}$$

$$\delta=\frac{1}{n(n-1)}\sum_{i=1}^{n}\sum_{j\neq i}^{n}\frac{\sqrt{\langle[r_{ij}(t)-\langle r_{ij}(t)\rangle_t]^2\rangle_t}}{\langle r_{ij}(t)\rangle_t} \tag{9}$$

δ is also known as the Lindemann parameter because the geometric information buried in it is analogous to that encountered in a bulk system. When the temperature is below the meltinglike transition, the cluster should behave very similar to a typical solid characterized by atoms oscillating around their equilibrium positions, and δ stays at a small and nearly constant value. If, on the contrary, δ changes drastically in some temperature range, it signals that the cluster could have undergone some kind of the structural or phasic transformation. For the purpose of quantitative analysis of the melting behavior of BCs and for the fact that BCs have the unique structural property of manifesting isomerization transitions involving permutational (in addition to topological) isomers, it is useful to record two additional sets of data.

The first set strikes at uncovering the temporal information upon which δ is calculated. To this end, it is instructive to rewrite Eq. (8) in an equivalent form

so that δ can be analyzed by following the trajectory of the instantaneous relative bond length $r_{ij}(t)$. At given temperature, the temporal development of r_{ij} permits insight into the microscopic dynamics of ij atoms (within the n-atoms cluster) of the same and different kinds. Strategically $r_{ij}(t)$ can be obtained as follows. For a BC maintained at given temperature, we effected Brownian MD simulations at $\Delta t=1-5\times10^{-15}$ s and run for a total simulation time of 3–10 ns. We calculated $r_{ij}(t)$ at every 100 Δt and collected $r_{ij}(t)$ altogether for a total number of $1-3\times10^4$.

The second set steers at constructing the temperature-dependent energy histograms and the use of them to supplement our understanding of $r_{ij}(t)$. To accomplish this, we run the simulation for 100 ns, after an equilibrium time of 25 ns. At any fixed temperature, we collected configurations from every 50 Δt increment. A total number of $2-10\times10^6$ configurations was stored. Starting with these atomic geometries which were treated as initial configurations, we applied the L-BFGS minimization algorithm[37] to locate their corre-

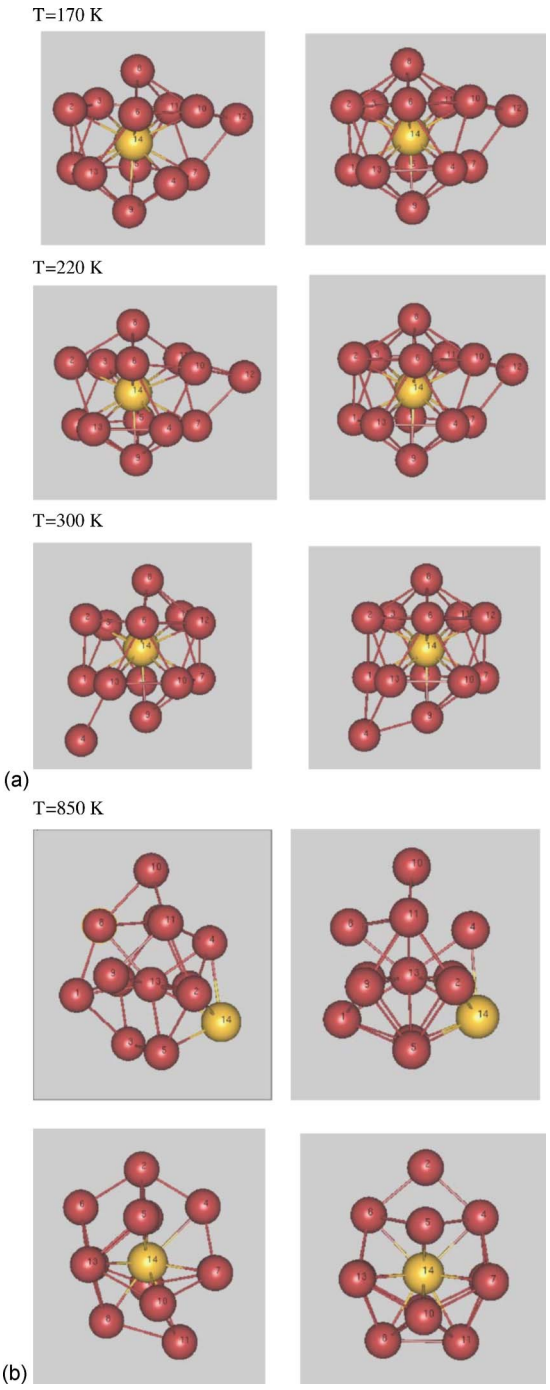

FIG. 7. (Color online) Selected atomic configurations of $Cu_{13}Au_1$ at temperatures (a) $T=170$ and 220 and 300 and (b) 850 K. The left column gives configurations at the instant captured whereas those on the right correspond to their local minima.

sponding local energy minima. The local energy minima of all these configurations were then recorded. Since the procedure was effected at each prescribed temperature, the distribution of the local energy minima yields the desired temperature-dependent energy histograms.

III. NUMERICAL RESULTS AND DISCUSSION

We present in Figs. 1(a), 1(b), 2, and 3 the temperature dependences of C_V and δ for Cu_mAu_{13-m} and Cu_mAu_{14-m}. In comparison with the same quantities obtained by López *et al.*[1] using constant energy simulations, the following general characteristics can be gleaned.

(1) Systematically, δ predicted in this work has its T_δ, which is the lowest energy point just before the first abrupt rise of δ, occurring at a distinctly lower temperature. This characteristic is seen for all of clusters Cu_mAu_{13-m} and Cu_mAu_{14-m}, as detailed in Table II. On the other hand, the melting temperatures T_{melt} for Cu_6Au_7 and Cu_7Au_7 which are deduced from the principal peak of C_V are predicted to locate at $k_BT_{\text{melt}} \approx 0.082$ eV and $k_BT_{\text{melt}} \approx 0.09$ eV, respectively. These T_{melt} are essentially indistinguishable from the only two simulation values reported by López *et al.* (see Table II). Furthermore, we find a prepeak at $k_BT \approx 0.054$ eV for Cu_7Au_7 and this value is also remarkably close to $k_BT \approx 0.05$ eV obtained by López *et al.*[1]

(2) As depicted in Fig. 3, the δ vs T curve for $Cu_{13}Au_1$ shows an anomalous characteristic in that it first increases almost vertically at $k_BT \approx 0.015$ eV, then maintains a nearly flat plateau up to $k_BT \approx 0.05$ eV ($T \approx 730$ K), and thereafter, it climbs up again to another plateau in a gradually increasing manner. In the same temperature range, C_V displays a well-developed prepeak whose onset is at $k_BT \approx 0.015$ eV and it is followed by a main peak located at the higher temperature $k_BT \approx 0.12$ eV.

Point (1) illuminates the systematic differences between simulation results obtained using the microcanonical and canonical ensembles that are applied to finite-sized clusters. These deviations are rather striking and the disparities are unquestionably in quest of an explanation. Considering the possible discrepancies in δ to arise from the use of different ensembles in finite systems, it is instructive to check first our Brownian-type MD simulation data which, in essence, describe a canonical ensemble, against standard canonical MC simulations. Two recent simulation works are available. Werner[38] calculated C_V and δ for Al_{13} employing exactly the same Gupta-like potential as Eq. (1) and independently Noya *et al.*[39] compared their simulation results for Al with experimentally observed data.[40] We portray in Fig. 4(a) our C_V and δ for Al_{13}. It is encouraging that both C_V and δ are in excellent agreement with those of Werner (see Fig. 3 in Ref. 38) who obtained these quantities from the standard canonical MC technique. Also, we display in Fig. 4(b) the C_V and δ simulated at size $n=58$ which is the only cluster exhibiting a clear prepeak at $T \approx 250$ K. For this cluster, our simulated C_V is also compatible to that obtained by Noya *et al.* (see Fig. 3 in Ref. 39) and to the experimental C_V value of Breaux *et al.* (see Fig. 2 in Ref. 40). As a further piece of evidence, we draw attention to a recent simulation work of Gallego *et al.*[41] who made a comparative study of the δ of Lennard-Jones heteroclusters. These authors scrutinized δ extracted from the MD and MC simulations performed in both the microcanonical and canonical ensembles. An interesting finding by the authors is the general trend of the $\delta-T$ curve which displays precisely the same trend as that shown in Table II between the present canonical ensemble simulations and the microcanonical ensemble simulations of López *et al.*[1]

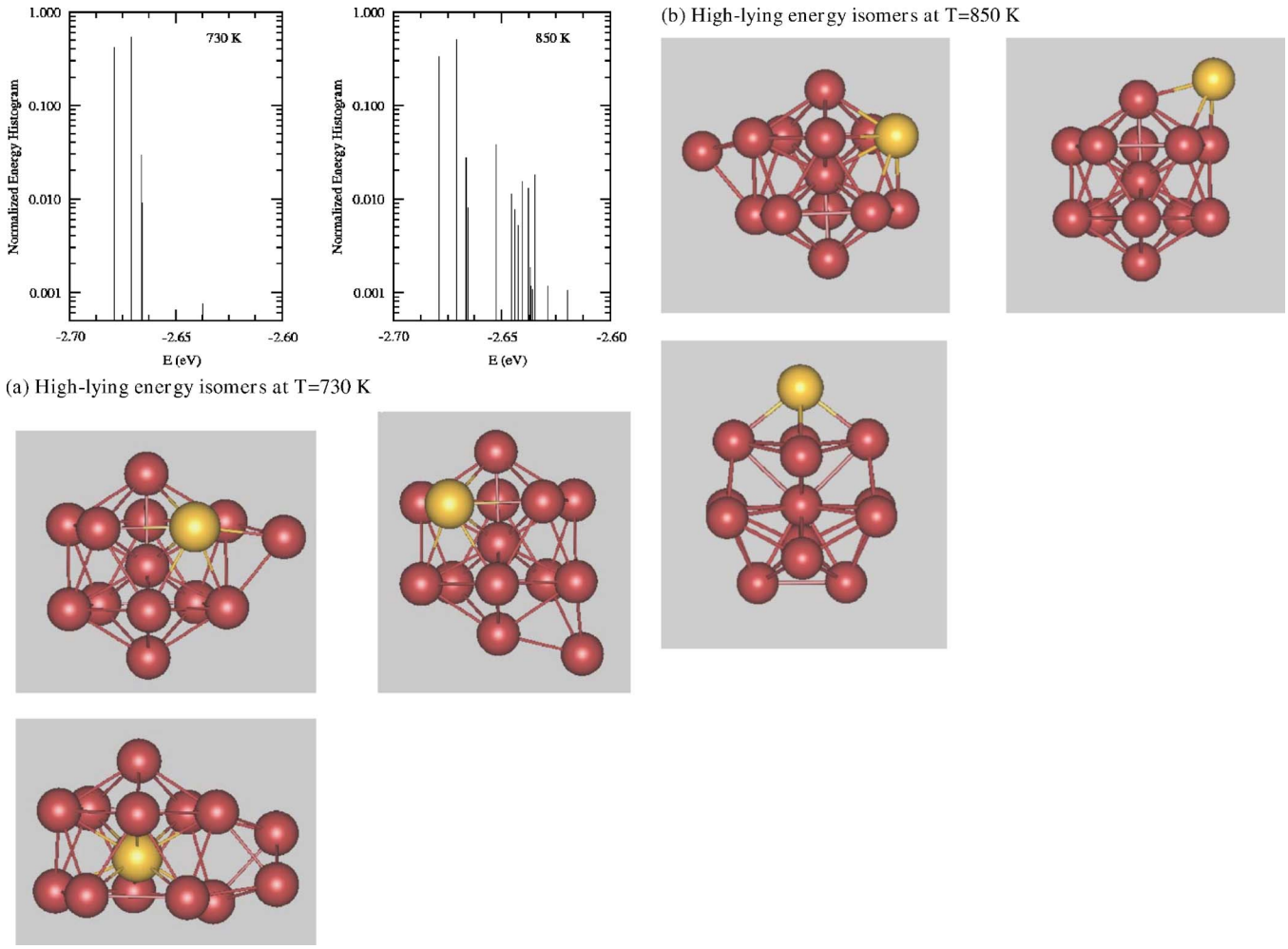

FIG. 8. (Color online) Energy histograms of $Cu_{13}Au_1$ obtained from Brownian MD simulations for the high-lying energy isomers at high temperatures (a) $T=730$ K and (b) $T=850$ K.

Point (2) is in need of further analysis. We show in Fig. 5 the normalized energy histograms and the lowest lying isomers for $Cu_{13}Au_1$. For $T<120$ K ($k_BT<0.01$ eV), δ mildly increases signaling solidlike vibrational behavior [Fig. 5(a)] and it climbs up almost vertically in an extremely small temperature interval of $\Delta T\approx 10$ K. Although there is a possibility that the cluster would make a isomerization transition involving topological isomers at the slightly higher temperature $T=160$ K [Fig. 5(b)], its occurrence is, however, negligibly low. Basically, the cluster is observed to stay in the solidlike lowest energy state with occasional permutations effected among the surface atoms Cu. The r_{ij} delineated in Fig. 6 (see, for instance, the case $T=170$ K) gives concrete evidence to support this atomic behavior. Further evidence can be gained by scrutinizing $r_{ij}(t)$ at $T=170$ K in greater detail. We note first of all that the lowest energy structure of $Cu_{13}Au_1$ is a 13-atom icosahedron with an atom "floating" at a site that lies between the apex position and the nearby pentagonal ring. The presence of a floating atom enhances the chance of the cluster executing isomerization transition involving permutational isomers. This permutational process, induced thermally, involves only Cu atoms either in the ground-state-like configuration [Fig. 5(a)] or in the first low-lying-like energy state whose configuration is topologically different [Fig. 5(b)]. At $T=170$ K, Fig. 6 (left column) shows one up rising step in r_{ij}. Here, one atom is the 12th floating atom and the other is the 7th or 10th Cu surface atom [see Fig. 7(a) for labels]. From the energy histograms given in Fig. 5, it is probable that the 7th or 10th Cu atom permutes with one other Cu surface atom causing an increment in r_{ij} and hence r_{ij} rises stepwisely. At this same temperature, there is no permutational transition between the central Au atom and the Cu atom. Neither do we notice any such kind of isomerization transition involving permutation among Cu surface atoms that do not contain the 12th floating Cu atom (right column in Fig. 6). Dynamically this would mean that, despite more frequent occurrence of the permutational transition or permutational transition involving topologically different isomers [Fig. 5(b)], the Au atom does not participate in the permutations but remains intact at its central position executing vibrational motion. It should be emphasized furthermore that the fluctuations in r_{ij} shown at $T=220$ and 300 K between the Au and Cu atoms (middle column in Fig. 6) are due to permutations of the 6th or 8th Cu atom with another atom either the surface or the floating Cu atom, and in the course of isomerization transition the 14th atom Au is residing all the time at the central position. Only at much

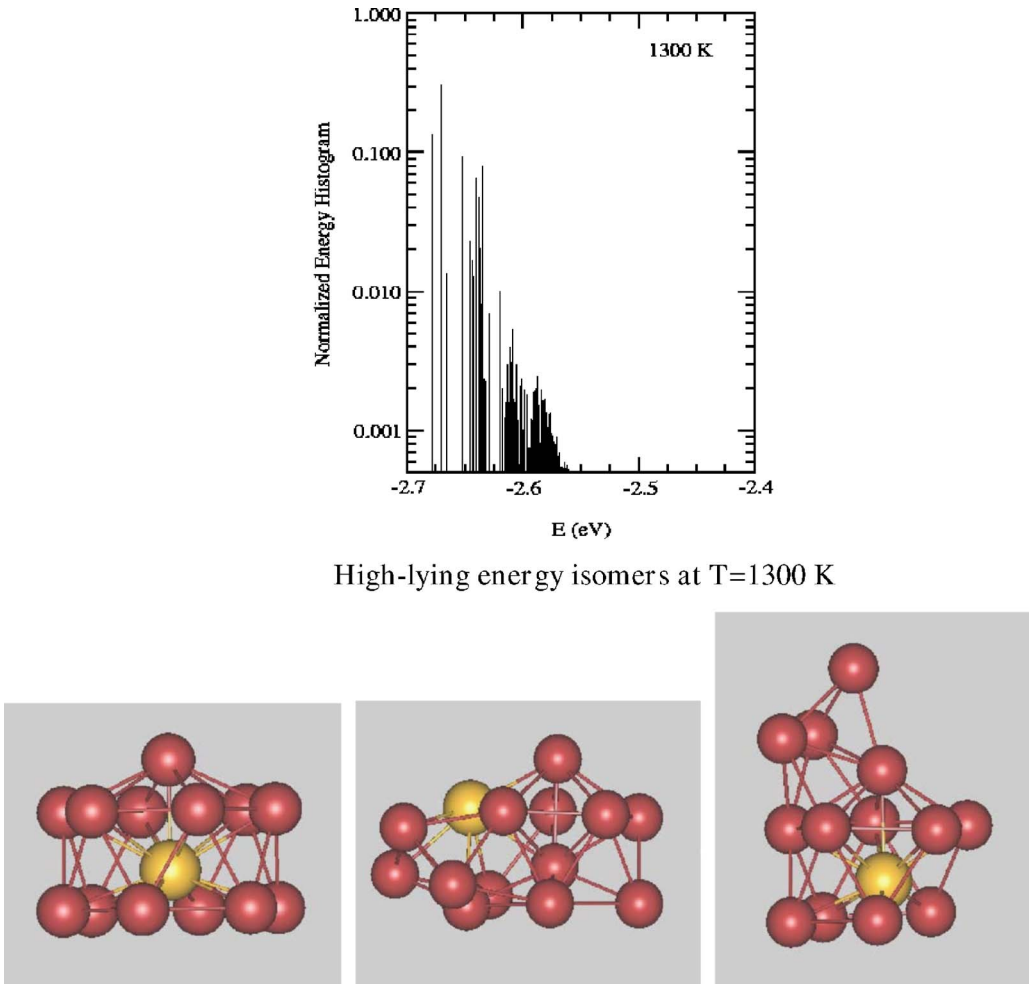

FIG. 9. (Color online) Same as Fig. 8 except for $Cu_{13}Au_1$ at $T=1300$ K.

higher temperatures $T \gtrsim 730$ K will one see the Au atom permutes with one of the Cu atoms. This characteristic feature is illuminated in Figs. 8(a), 8(b), and 9 where the energy histograms and their associated high-lying energy isomers are depicted. Notice that the r_{ij} that contains the central Au atom (middle column in Fig. 6) at $T=850$ K fluctuates up indicating that there is a isomerization transition now involving permutational isomers in which are seen the Au atom leaving the central location [Figs. 7(b) and 8(b)]. In fact, the cluster around $T \approx 850$ K has already shown a sign of disordered structure [see Fig. 7(b)]. At the much higher temperature $T=1300$ K, the cluster has undoubtedly been driven into a liquidlike state (Fig. 9) since much larger fluctuations in r_{ij} are observed (Fig. 10). It is now obvious that underlying the temperature dependences of δ is the rather complicated isomerization transitions among the Au and Cu atoms. If, in response to temperature, the isomerization transition involving permutational or topological isomers were taken place with the cluster preserving the "solidlike " structure, $\delta(T)$ will then have no bearing on the usual notion of "solidlike-liquidlike " melting. It is therefore not surprising to see the incongruity between the $C_V(T)$ on one hand and the $\delta(T)$, on the other hand; the disparity between them can thus be understood not only from the larger energy fluctuations occurring in canonical ensemble simulations, as pointed out by Werner,[38] but also by the complex behavior of isomerization transitions such as those brought about by the floating atom.

IV. CONCLUSION

The Brownian-type MD simulation was applied to study the temperature dependence of BCs. We make a direct comparison between the simulation results for the specific heat C_V and the rms relative bond length fluctuation parameter δ calculated in the present canonical ensemble simulations and those performed by the microcanonical ensemble simulations. We observed systematic deviations in the results obtained from these two sources, and the differences are alluded to the use of different ensembles in a finite-sized system. For the disparity generally found between C_V and δ as a function of temperature, we examine the temporal behavior of the instantaneous bond length fluctuation $r_{ij}(t)$. We find that information on the isomerization transitions involving permutational and topological isomers may be obtained by examining the temporal change of $r_{ij}(t)$ and hence $\delta(T)$. With detailed analysis of the time behavior of $r_{ij}(t)$ supplemented by the energy histograms, we can now understand better the incongruity of $C_V(T)$ and $\delta(T)$. We conclude by summarizing further two main features that come into play.

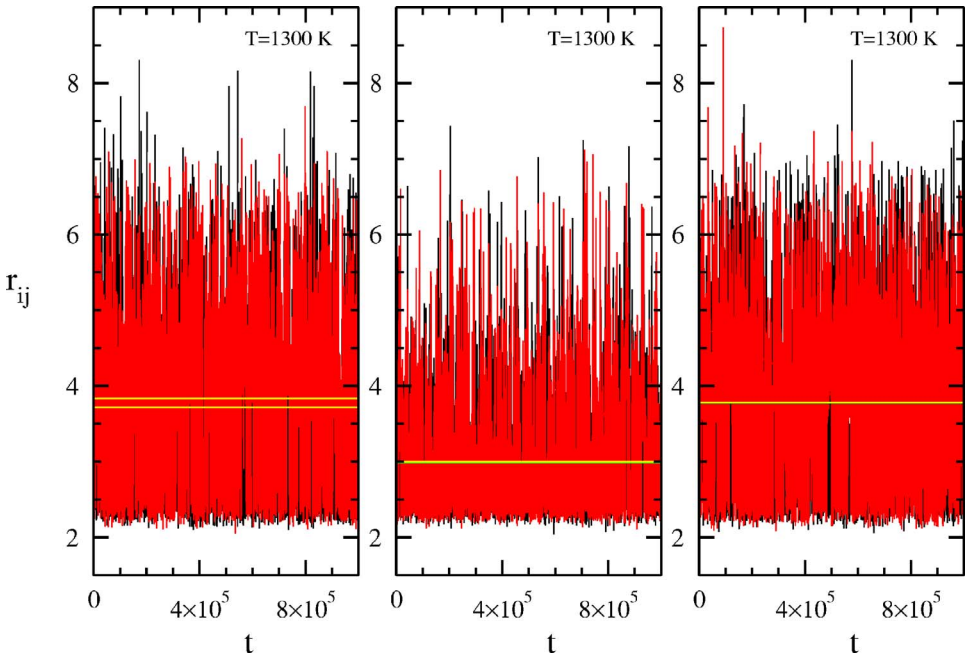

FIG. 10. (Color online) Instantaneous bond length $r_{ij}(t)$ calculated from Brownian MD simulations for $Cu_{13}Au_1$ at $T=1300$ K. The left and right columns describe r_{ij} where the ith and jth are Cu surface atoms whereas the middle column has one of ij atoms of r_{ij} the central Au atom (ith or jth). The horizontal lines (green for black r_{ij} and yellow for red r_{ij}) in each figure refer to $\langle r_{ij}(t)\rangle_t$.

(1) For BCs Cu_mAu_{13-m} and Cu_mAu_{14-m}, the T_δ of δ deduced from simulations in canonical and microcanonical ensembles shows systematic differences, and they are given in Table II. The T_{melt} of C_V, on the contrary, is almost the same for the BCs considered here.

(2) It appears that clusters with a "floating" atom in the lowest energy structure are more susceptible to an isomerization transition involving permutational isomers. The presence of such a "floating" atom may also induce topological changes with other surface atoms involved, and it leads to the peculiar feature of δ as seen in Cu_mAu_{14-m} including the case Cu_{14} (not shown in this work).

ACKNOWLEDGMENTS

We acknowledge the financial support (NSC 95-2112-M-008-036) from the National Science Council, Taiwan, ROC.

*Electronic address: sklai@coll.phy.ncu.edu.tw
†Present address: Laboratoire de Thermodynamique et physico-Chimie Métallurgique, 1130, rue de la Piscine, Domaine Universitaire, BP 75, 38402 St Martin d'Hères, cedex, France.

[1] M. J. López, P. A. Marcos, and J. A. Alonso, J. Chem. Phys. **104**, 1056 (1996).
[2] C. Rey, J. Garcia-Rodeja, and L. J. Gallego, Phys. Rev. B **54**, 2942 (1996).
[3] J. Jellinek and E. B. Krissinel, Chem. Phys. Lett. **258**, 283 (1996).
[4] E. B. Krissinel and J. Jellinek, Chem. Phys. Lett. **272**, 301 (1997); , Int. J. Quantum Chem. **62**, 185 (1997).
[5] A. F. Voter and S. P. Chen, in *Characterization of Defects in Materials*, edited by R. W. Siegal, J. R. Weertman, and R. Sinclair, MRS Symposia Proceedings No. 82 (Materials Research Society, Pittsburgh, 1987), p. 175.
[6] R. P. Gupta, Phys. Rev. B **23**, 6265 (1981).
[7] F. Cleri and V. Rosato, Phys. Rev. B **48**, 22 (1993).
[8] M. Calleja, C. Rey, M. M. G. Alemany, L. J. Gallego, P. Ordejón, D. Sánchez-Portal, E. Artacho, and J. M. Soler, Phys. Rev. B **60**, 2020 (1999).
[9] E. F. Rexer, J. Jellinek, E. B. Krissinel, E. K. Parks, and S. J. Riley, J. Chem. Phys. **117**, 82 (2002).
[10] J. Wang, G. H. Wang, X. S. Chen, W. Lu, and J. Zhao, Phys. Rev. B **66**, 014419 (2002).
[11] S. Darby, T. V. Mortimer-Jones, R. L. Johnston, and C. Roberts, J. Chem. Phys. **116**, 1536 (2002).
[12] R. A. Lordeiro, F. F. Guimarães, J. C. Belchior, and R. L. Johnston, Int. J. Quantum Chem. **95**, 112 (2003).
[13] G. Rossi, A. Rapallo, C. Mottet, A. Fortunelli, F. Baletto, and R. Ferrando, Phys. Rev. Lett. **93**, 105503 (2004).
[14] A. Rapallo, G. Rossi, R. Ferrando, A. Fortunelli, B. C. Curley, L. D. Lloyd, G. M. Tarbuck, and R. L. Jonnston, J. Chem. Phys. **122**, 194308 (2005); **122**, 194309 (2005).
[15] F. Baletto, C. Mottet, and R. Ferrando, Phys. Rev. B **66**, 155420 (2002); , Phys. Rev. Lett. **90**, 135504 (2003).
[16] M. S. Bailey, N. T. Wilson, C. Roberts, and R. L. Johnston, Eur. Phys. J. D **25**, 41 (2003).
[17] P. J. Hsu and S. K. Lai, J. Chem. Phys. **124**, 044711 (2006).
[18] G. E. Lopez and D. L. Freeman, J. Chem. Phys. **98**, 1428 (1993).
[19] S. P. Huang and P. B. Balbuena, J. Phys. Chem. B **106**, 7225 (2002).
[20] Subramanian K. R. S. Sankaranarayanan, Venkat R. Bhethanabotla, and Babu Joseph, Phys. Rev. B **71**, 195415 (2005).
[21] K. Michaelian and I. L. Garzón, Eur. Phys. J. D **34**, 183 (2005).
[22] D. Cheng, S. Huang, and W. Wang, Eur. Phys. J. D **39**, 41 (2006).
[23] S. K. Lai, W. D. Lin, K. L. Wu, W. H. Li, and K. C. Lee, J. Chem. Phys. **121**, 1487 (2004).

[24] M. Bixon and J. Jortner, J. Chem. Phys. **91**, 1631 (1989).
[25] S. Nosé, J. Chem. Phys. **81**, 511 (1984); , Mol. Phys. **52**, 255 (1984).
[26] W. G. Hoover, Phys. Rev. A **31**, 1695 (1985); H. A. Posch, W. G. Hoover, and F. J. Vesely, *ibid.* **33**, 4253 (1986).
[27] D. Kusnezov, A. Bulgac, and W. Bauer, Ann. Phys. (N.Y.) **204**, 155 (1990); A. Bulgac and D. Kusnezov, Phys. Rev. A **42**, 5045 (1990).
[28] A. Bulgac and D. Kusnezov, Phys. Rev. Lett. **68**, 1335 (1992); , Phys. Rev. B **45**, 1988 (1992).
[29] A. Bulgac and D. Kusnezov, Phys. Lett. A **151**, 122 (1990).
[30] N. Ju and A. Bulgac, Phys. Rev. B **48**, 2721 (1993); See also Ref. 25; W. G. Hoover, *Molecular Dynamics, Lecture Note in Physics* (Springer, New York, 1986), Vol. 258. The advantages of the present scheme over the usual Nosé-Hoover type of coupling (Refs. 25 and 26) or its generalizations (Ref. 27) are discussed at length in this reference to which the interested readers are referred.
[31] G. Martyna, M. Klein, and M. Tuckerman, J. Chem. Phys. **97**, 2635 (1992).
[32] The correct selection of the thermostatting parameter such as the auxiliary function coefficient [B. J. Leimkuhler and C. R. Sweet, J. Chem. Phys. **121**, 108 (2004)], thermostatting mass, etc., even for simple model systems remains to be experimented before any quantitative application.
[33] B. J. Leimkuhler and C. R. Sweet, SIAM J. Appl. Dyn. Syst. **4**, 187 (2005).
[34] S. Bond, B. Laird, and B. J. Leimkuhler, J. Comput. Phys. **151**, 114 (1999).
[35] C. H. Chien, E. Blaisten-Barojas, and M. R. Pederson, J. Chem. Phys. **112**, 2301 (2000).
[36] C. Borgs and R. Kotecky, J. Stat. Phys. **79**, 43 (1995).
[37] D. Liu and J. Nocedal, Math. Program. **45**, 503 (1989).
[38] R. Werner, Eur. J. Phys. **43**, 47 (2005).
[39] E. G. Noya, J. P. K. Doye, and F. Calvo, Phys. Rev. B **73**, 125407 (2006).
[40] G. A. Breaux, C. M. Neal, B. Cao, and M. F. Jarrold, Phys. Rev. Lett. **94**, 173401 (2005).
[41] L. J. Gallego, M. J. Grimson, and C. Rey, Phys. Rev. B **51**, 5518 (1995).